The nature of hydrogen-related fracture in X80 pipeline steel with stress concentration

T Homma[1], S Onuki[2], H Suzuki[3] and K Takai[3]

[1]Graduate School of Science and Technology, Sophia University, 7-1 Kioi-cho, Chiyoda-ku, Tokyo 102-8554, Japan
[2]Tokyo Gas Co., Ltd., 1-7-7, Suehiro-cho, Tsurumi-ku, Yokohama, Kanagawa 230-0045, Japan
[3]Faculty of Science and Technology, Department of Engineering and Applied Sciences, Sophia University, Tokyo, Japan

E-mail: t-homma-fc4@eagle.sophia.ac.jp

Abstract. The nature of hydrogen-related fracture in X80 pipeline steel with stress concentration was investigated through observation of fracture modes at hydrogen-related crack initiation sites and crystallographic analysis of fracture surfaces. The fracture modes and crack initiation sites were observed using a field emission scanning electron microscope (FE-SEM). The hydrogen-related crack initiation sites of X80 specimens were quasi-cleavage (QC) fracture at the notch tip. In addition, distributions of plastic strain and principal stress near the notch tip were calculated by finite element method (FEM) analysis. Since maximum plastic strain occurred at the notch tip where the initiation of QC fracture was observed, the main factor causing QC fracture was probably plastic strain. In order to clarify the crystallographic features of hydrogen-related fracture surfaces of X80, a trace analysis of the QC fracture surface was carried out using electron backscatter diffraction patterns (EBSD). Since not all points on the fracture surface were parallel to {011} slip planes, hydrogen-related fracture consisted of not only {011} slip planes but also various crystal planes due to cross slip in the body-centered cubic lattice. These findings indicate that the nature of hydrogen-related fracture in X80 is probably associated with plastic strain on various slip planes.

1 Introduction

For the development of the hydrogen economy, transport of hydrogen using gas pipelines would enable it to be transported in large quantities at low cost. However, hydrogen embrittlement is a concern when large earthquakes occur that can induce large strain in pipelines. Hattori et al. evaluated hydrogen embrittlement susceptibility using smooth specimens of X80 pipeline steel and reported that hydrogen-enhanced strain-induced lattice defects are involved in the reduction of ductility [1]. However, corrosion pits and scratches may exist on the pipeline surface in an actual environment, so it is more important to investigate hydrogen embrittlement susceptibility and the fracture mechanism of X80 under stress concentration. Therefore, in the present study, the effect of the hydrogen content and tensile rate on hydrogen embrittlement susceptibility was investigated along with examining the nature of hydrogen-related fracture in X80 under stress concentration.

IOP Conf. Series: Materials Science and Engineering **461** (2019) 012025 doi:10.1088/1757-899X/461/1/012025

2 Experimental

2.1 Materials

X80 pipeline steel with a ferrite-bainite microstructure was used in the present study. The detailed chemical composition of this steel is shown in Table 1. Specimens with gauge dimensions of 20 × 10 × 2.0 mm were machined from actual pipelines. Notches (K_t i.e., the stress concentration factor: 3.6) were introduced in the center of the specimen gauge region as locations of stress concentration.

2.2 Hydrogen embrittlement susceptibility

The first set of tensile tests was carried out to investigate the influence of hydrogen content. Specimens were electrochemically precharged with hydrogen in an aqueous solution of 0.1 N NaOH and from 0 to 10 $g \cdot l^{-1}$ NH_4SCN with a current density of 5 $A \cdot m^{-2}$ for 72 h. Hydrogen content was measured by thermal desorption analysis (TDA) at a heating rate of 100 ºC$\cdot h^{-1}$. Tensile tests were carried out at a crosshead speed of 0.05 $mm \cdot min^{-1}$ at 30 ºC. The second set of tensile tests was carried out by changing the crosshead speed. Specimens were electrochemically precharged with hydrogen in an aqueous solution of 0.1 N NaOH and 1 $g \cdot l^{-1}$ NH_4SCN with a current density of 5 $A \cdot m^{-2}$ for 72 h. Tensile tests were carried out at a crosshead speed of 0.005-1 $mm \cdot min^{-1}$ at 30 ºC with/without hydrogen precharging. Hydrogen charging was conducted concurrently with the tensile tests after precharging in order to keep the hydrogen content constant. For the uncharged specimens, the tensile tests were conducted in air at 30 ºC. Hydrogen embrittlement susceptibility was evaluated based on the maximum fracture strength.

2.3 Controlling factor of crack initiation induced by hydrogen

The crack initiation site of hydrogen-related fracture in X80 was investigated based on the method reported by Kurokawa et al. [2]. The load was applied with hydrogen charging and unloaded just before fracture. After unloading, the samples were kept in a thermostatic chamber in air at 30 ºC for 144 h for degassing and tensile testing was conducted at a crosshead speed of 0.05 $mm \cdot min^{-1}$ in air. Hydrogen-related crack initiation sites of fracture surfaces were observed with a field emission scanning electron microscope (FE-SEM). Furthermore, the ABAQUS modeling software was used to conduct a simulation of the distribution of principal stress and plastic strain in the vicinity of the notch root.

2.4 Crystallographic analysis of fracture surface at hydrogen-related crack initiation site

A trace analysis was carried out using electron backscatter diffraction patterns (EBSD) to clarify the crystallographic features of hydrogen-related fracture surfaces of X80. A Ni layer was electrodeposited onto the tensile-tested hydrogen-charged specimen with an aqueous solution of 50 $g \cdot L^{-1}$ Ni_2SO_4 + 15 $g \cdot L^{-1}$ NH_4Cl + 15 $g \cdot L^{-1}$ H_3BO_4 to preserve the fracture surface. One side of the electrodeposited specimen was mechanically polished and then polished with colloidal silica. The EBSD measurement and analysis were performed with TSL OIM Data Collection and TSL OIM Analysis, respectively.

Table 1. Chemical composition of X80 steel.

Element	C	Si	Mn	P	S	Nb	Mo	Ti
wt. %	0.08	0.22	1.85	0.007	0.002	0.05	0.12	0.02

IOP Conf. Series: Materials Science and Engineering **461** (2019) 012025 doi:10.1088/1757-899X/461/1/012025

3 Results and discussion

3.1 Hydrogen embrittlement susceptibility

Figure 1 shows the relationship between the maximum fracture strength and hydrogen content. As the hydrogen content increased, the maximum fracture strength decreased and then became constant. Figure 2 shows the relationship between the maximum fracture strength and the crosshead speed. As the crosshead speed decreased, the maximum fracture strength decreased only for hydrogen-charged specimens, resulting in increased hydrogen embrittlement susceptibility. Possible causes of these results are the hydrogen concentration in a stress concentrated region and the interaction between dislocations and hydrogen. During the tensile test, hydrogen accumulated at the notch tip due to stress-induced diffusion. At a low crosshead speed, hydrogen accumulated sufficiently because there was ample time for it to diffuse [3]. In addition, at a low crosshead speed, hydrogen can move with moving dislocations and the interaction between dislocations and hydrogen is expected to have a large effect [4].

3.2 Controlling factor of crack initiation induced by hydrogen

Figure 3 shows a photograph of crack initiation sites of a fracture surface at the notch tip of a hydrogen-charged specimen to which the load was applied until just before fracture; the specimen was then dehydrogenated and fractured in the air. Figure 3 (a) shows QC fracture at the notched tip region and microvoid coalescence (MVC) inside specimen. Furthermore, Figure 3 (b) shows QC fracture surface in high magnification. Figure 4 shows the distribution of principal stress and plastic strain at the notch tip obtained by FEM analysis. The plastic strain was maximum at the notch root and the principal stress was maximum at about 0.13 mm away from the notch root. QC fracture is observed in the region from the notch root to about 75 μm away in Figure 3, and this region does not include the maximum principal stress point. Therefore, the main factor causing QC fracture was probably plastic strain.

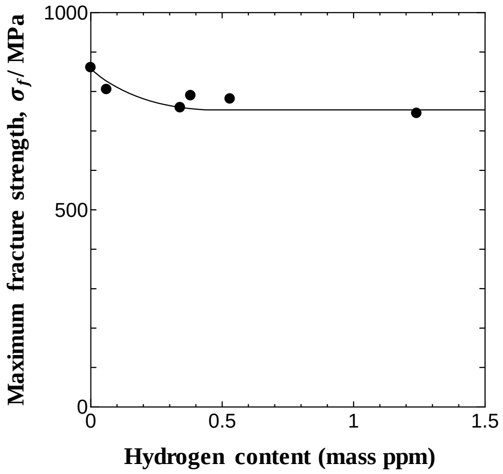

Figure 1. Relationship between maximum fracture strength and hydrogen content.

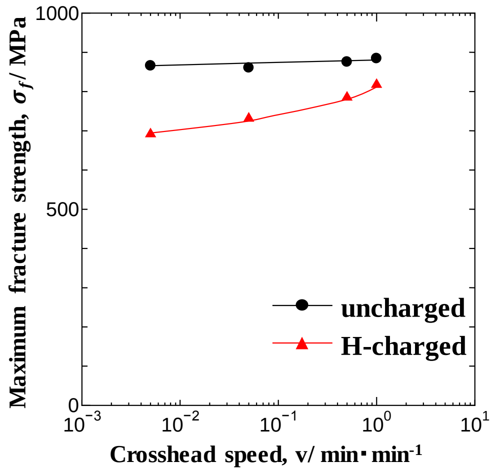

Figure 2. Relationship between maximum fracture strength and crosshead speed.

IOP Conf. Series: Materials Science and Engineering **461** (2019) 012025 doi:10.1088/1757-899X/461/1/012025

3.3 Crystallographic analysis of fracture surface at hydrogen-related crack initiation site

Figure 5 shows (a) an SEM image and (b) an EBSD orientation map of the QC fracture surface caused by hydrogen. The light gray area in the SEM image and the black area in the EBSD orientation map correspond to the Ni layers. The orange line in the SEM image shows the boundary on the first surface and the blue line shows the boundary on the second surface. The lengths of the white bars show the calculated translation distance values. The traces of {011} planes and cubic lattices showing crystal orientation near the fracture surface are indicated by the red lines in the EBSD orientation map. The measurement point numbers parallel to the {011} planes are indicated in red, and the measurement point numbers not parallel to the {011} planes are indicated in white. The measurement points parallel to the {011} planes are 3/16 points. Since not all points on the fracture surface are parallel to {011} slip planes, hydrogen-related fracture probably consisted of not only {011} slip planes but also various crystal planes due to cross slip in the body-centered cubic lattice.

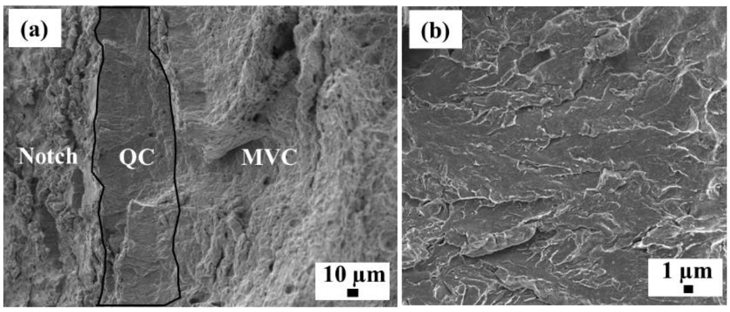

Figure 3. Crack initiation sites of fracture surface at the notch tip in (a)low magnification and (b)high magnification of QC fracture.

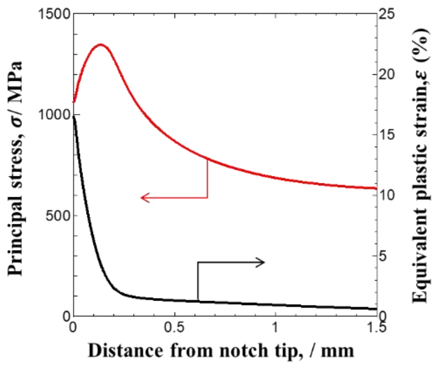

Figure 4. Distribution of principal stress and equivalent plastic strain at the notch tip.

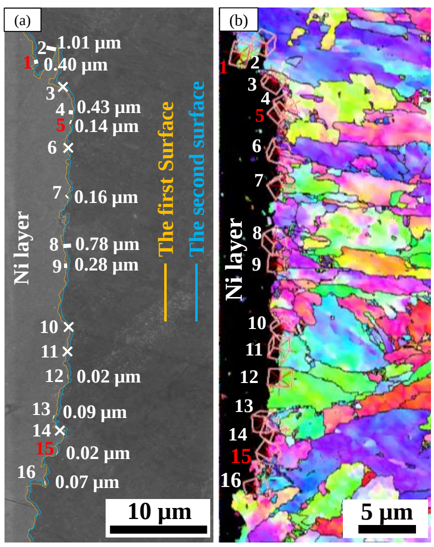

Figure 5. (a) SEM image and (b) EBSD orientation map of quasi-cleavage fracture surface caused by hydrogen.

4 Conclusion

The nature of hydrogen-related fracture in X80 pipeline steel with stress concentration was investigated through observation of fracture modes at the hydrogen-related crack initiation sites and crystallographic analysis of fracture surfaces. The results can be summarized as follows.

(1) Hydrogen embrittlement susceptibility increased with increasing hydrogen content and decreasing crosshead speed.

(2) The hydrogen-related crack initiation sites of X80 specimens were QC fracture at the notch tip. Plastic strain was maximum at the notch root and the principal stress was maximum at about 0.13 mm away from the notch root. Therefore, the main factor causing QC fracture was probably plastic strain.

(3) QC fracture in X80 consisted of not only {011} slip planes but also various crystal planes.

References

[1] Hattori M, Suzuki H, Seko Y and Takai K 2017 The role of hydrogen-enhanced strain-induced lattice defects on hydrogen embrittlement susceptibility of X80 pipeline steel *The journal of the Minerals, Metals & Materials Society* **69** 1375-1380.

[2] Kurokawa A, Doshida T, Hagihara Y, Suzuki H and Takai K 2017 Main factors causing intergranular and quasi-cleavage fractures at hydrogen-induced cracking in tempered martensitic steels Proc. Int. Conf.on the Science and Engineering of Materials (Kuala Lumpur:Malaysia) **1958** 020027-1–020027-9

[3] Wang M, Akiyama E and Tsuzaki K, 2005 Crosshead speed dependence of the notch tensile strength of a high strength steel in the presence of hydrogen *Scripta Materialia* **53** 713–718.

[4] Shoda H, Suzuki H, Takai K and Hagihara Y 2010 Hydrogen Desorption Behavior of Pure Iron and Inconel 625 during Elastic and Plastic Deformation *ISIJ International* **50** 115-123